CANCER RESEARCH | PRIORITY REPORT

SLC43A3 Is a Biomarker of Sensitivity to the Telomeric DNA Damage Mediator 6-Thio-2′-Deoxyguanosine

Ilgen Mender[1], Kimberly Batten[1], Michael Peyton[2], Aishwarya Vemula[1], Crystal Cornelius[1], Luc Girard[2,3,4], Boning Gao[2,3], John D. Minna[2,3,4,5], and Jerry W. Shay[1]

ABSTRACT

Cell membrane transporters facilitate the passage of nucleobases and nucleosides for nucleotide synthesis and metabolism, and are important for the delivery of nucleoside analogues used in anticancer drug therapy. Here, we investigated if cell membrane transporters are involved in the cellular uptake of the nucleoside analogue DNA damage mediator 6-thio-2′-deoxyguanosine (6-thio-dG). A large panel of non–small cell lung cancer (NSCLC) cell lines (73 of 77) were sensitive to 6-thio-dG; only four NSCLC lines were resistant to 6-thio-dG. When analyzed by microarray and RNA sequencing, the resistant NSCLC cell lines clustered together, providing a molecular signature for patients that may not respond to 6-thio-dG. Significant downregulation of solute carrier family 43 A3 (SLC43A3), an equilibrative nucleobase transporter, was identified as a candidate in this molecular resistance signature. High levels of SLC43A3 mRNA predicted sensitivity to 6-thio-dG and therefore SLC43A3 could serve as a promising biomarker for 6-thio-dG sensitivity in patients with NSCLC.

Significance: These findings identify a biomarker of resistance to the telomeric DNA damage mediator 6-thio-2′-deoxyguanosine.

Introduction

Nucleosides (nucleobase, ribose or deoxyribose) and their related nucleotides (nucleobase, ribose or deoxyribose and phosphate) are the key building blocks of DNA and RNA. The de novo materials of purine synthesis are amino acids and bicarbonate, whereas the salvage pathway utilizes nucleobases from the degradation of nucleosides and nucleotides to assemble newly synthesized nucleotides. The salvage pathway saves energy for nucleotide production (1–3). Molecules such as purine nucleobases that cannot permeate membranes by simple diffusion utilize biological transport systems to pass through the plasma membrane. Several solute carrier (SLC) transporters have been identified for the transport of purine nucleobases such as concentrative and facilitative transporters [sodium-dependent nucleobase transporter 1 (SNBT1/SLC23A4), equilibrative nucleoside transporter 1 (ENT1/SLC29A1, ENT2/SLC29A), and equilibrative nucleobase transporter 1 (ENBT1/SLC43A3); reviewed in ref. 4]. SLC43A3 is a member of the SLC43A family comprising two other members SLC43A1 and SLC43A2, which mediate facilitative transport of neutral amino acids (5). SLC43A3 is a nucleobase transporter involved in purine salvage pathways in mammals (6) and has a potential role in delivering the structural analogues of nucleobases, such as anticancer (6-thio-guanine, 6-mercaptopurine) and antiviral (acyclovir, ganciclovir)

drugs (4, 7). Although acyclovir and ganciclovir (2′-deoxyguanosine analogues) lack a sugar ring, they still act as nucleosides (8). SLC43A3 is highly expressed in several embryonic epithelial tissues such as lung and liver and was also named embryonic epithelial gene 1 (4).

6-Thio-2′-deoxyguanosine (6-thio-dG) is a modified purine nucleoside analogue prodrug that is preferentially incorporated into telomeres but only in telomerase-positive cells, leading to telomere uncapping, genomic instability, and cell death, with minimal cytotoxic effects on telomerase-negative normal cells. In addition, 6-thio-dG is effective and safe in mice (9, 10). Recently, we demonstrated that 6-thio-dG overcomes EGFR-targeted and platin-doublet chemotherapy resistance in non–small cell lung cancer (NSCLC) cell lines (11); therapy-resistant pediatric brain cancers (12); targeted therapy (PLX4720 BRAF inhibitor) resistance in melanomas (13); and immunotherapy (checkpoint inhibitor) resistance in melanomas (13). In addition, 6-thio-dG in combination with gamitrinib showed improved results in "untargetable" NRAS oncogene–induced melanoma (14). Thus, there is an urgent need for additional therapeutic options for multidrug resistant tumors. In the present preclinical studies, based on a candidate approach from transcriptomic analyses on 6-thio-dG–sensitive and –resistant cell lines, we tested if the SLC43A3 transporter is involved in the cellular uptake of 6-thio-dG. We found that approximately 95% of NSCLC cell lines tested are sensitive to 6-thio-dG and contain very high levels of SLC43A3 mRNA while resistant cells have significantly lower levels of SLC43A3 providing a potential biomarker of intrinsically resistant cell lines. Mechanistically, we found that human lung cancer cells that are resistant to 6-thio-dG expressed low mRNA levels of the SLC43A3 transporter gene. Experimental manipulation of SLC43A3 levels altered the sensitivity of cells to 6-thio-dG. In addition, treatment with increasing doses of 6-thio-dG resulted in resistance to 6-thio-dG that correlated with reduced levels of SLC43A3. In summary, SLC43A3 expression levels may predict the efficacy of 6-thio-dG in patients with multidrug resistant NSCLC.

[1]Department of Cell Biology, University of Texas Southwestern Medical Center, Dallas, Texas. [2]Hamon Center for Therapeutic Oncology Research, University of Texas Southwestern Medical Center, Dallas, Texas. [3]Simmons Comprehensive Cancer Center, UT Southwestern Medical Center, Dallas, Texas. [4]Department of Pharmacology, UT Southwestern Medical Center, Dallas, Texas. [5]Department of Internal Medicine, UT Southwestern Medical Center, Dallas, Texas.

Corresponding Author: Jerry W. Shay, UT Southwestern Medical Center, 6000 Harry Hines Boulevard, Dallas, TX 75930-9039. Phone: 214-648-4201; Fax: 214-648-5814; E-mail: jerry.shay@utsouthwestern.edu

Materials and Methods

Cell lines

The NCI and Hamon Cancer Center (HCC) at UT Southwestern series of lung cancer cell lines used in this study were obtained from the

UT Southwestern Hamon Center repository. Except when noted, mycoplasma-free (e-Myco kit, Boca Scientific) human cancer cell lines were grown in a Medium X (DMEM:199, 4:1, Hyclone) supplemented with 10% cosmic calf serum (Hyclone) without antibiotics and incubated with 5% CO_2 at 37°C. NSCLC and SCLC cell lines were authenticated using the Power-Plex 1.2 kit (Promega) that matched the DNA fingerprint library maintained by the ATCC. Patient-derived NSCLC cells were grown in RPMI-1640 (Sigma) supplemented with 5% cosmic calf serum incubated in low oxygen (2%–3%) at 37°C.

Drug preparation

For *in vitro* studies, 6-thio-dG (Metkinen Oy) was dissolved in DMSO/water (1:1) to prepare 10 mmol/L stock solutions, and maintained at −20°C. A 1 mmol/L final concentration stock was prepared for *in vitro* experiments and added in fresh medium at different concentrations for cell treatments. For *in vivo* studies, 3 mg/kg 6-thio-dG was prepared in 5% DMSO (in 1xPBS) and kept frozen at −20°C.

Cell viability assay

For determination of IC_{50} with cell proliferation assays, a panel of human NSCLC and SCLC was screened with 6-thio-dG with a 2- to 4-fold dilution series in 8 different points in 96-well plates. Cells were plated 24 hours prior to addition of drug, incubated for 4 days, and assayed using the CellTiter 96 Aqueous One Solution Cell Proliferation Assay (Promega). Dose–response curves were generated and IC_{50}s calculated using in-house software, DIVISA or Graphpad Prism. All samples were analyzed in triplicate, and SDs were from 2 to 3 independent experiments. For determination of viable cells, H1693 and H1693 *SLC43A3*-overexpressed cells (5,000 cells/cm^2) and H2087 clones (3,000 cells/cm^2) were treated with 10 μmol/L 6-thio-dG for 4 to 7 days and then counted.

Transient siRNA experiments

For siRNA experiments, HCC4017 NSCLC cell lines were either plated in 96-well plates (3,000 cells per well) to determine cell viability or 6-well plates (200,000 cells per well) to determine knockdown efficiency. Cells were reverse-transfected with nonsilencing controls (Santa Cruz Biotechnology, sc-37007) or a pool of three different siRNA duplexes targeting *SLC43A3* (Santa Cruz Biotechnology, sc-96371).

sc-96371A, sense RNA sequence: 5′- CCUUCAUCCUGCAAGU-GAUtt-3′, antisense RNA sequence: 5′-AUCACUUGCAGGAU-GAAGGtt-3′,

sc-96371B, sense RNA sequence: 5′- CCAUCUUCACCCUCAU-CAAtt-3′, antisense RNA sequence: 5′- UUGAUGAGGGUGAA-GAUGGtt-3′,

sc-96371C, sense RNA sequence: 5′- GUUGCCAAGCAGAUU-GAUAtt-3′, antisense RNA sequence: 5′- UAUCAAUCUGCUUGG-CAACtt-3′.

Transfection siRNA complexes (70 nmol/L) were prepared using OptiMEM (Invitrogen) and RNAimax (Invitrogen). For knockdown efficiency, following 72 hours of exposure to siRNAs, cells were washed, trypsinized, counted, and pelleted for RNA extraction. For cell viability assays, 48 hours after transfection, cells were treated with 6-thio-dG with a 2-fold dilution series in 18 different points in 96-well plates. Seventy-two hours later, dose–response curves were generated and IC_{50}s calculated.

Transfection, lentivirus production, and infection

SLC43A3 cDNA was inserted into pLenti6/V5_GW/lacZ (Invitrogen) and cotransfected with packaging vectors pMD2.G (Addgene,

12259) and psPAX2 (Addgene, 12260) in 90% confluent 293FT cells for viral production. Note that 10 μg of plasmid DNA and 20 μL of Lipofectamine 2000 (Invitrogen) were used for transfections. Supernatant lentiviral containing medium was concentrated with Lenti-X concentrator solution (Takara, 631231).

Reverse transcriptase and droplet digital PCR

RNA was isolated using RNeasy Plus Mini Kit (Qiagen, 74134) and stored at −80°C. cDNAs were synthesized using the iScript cDNA Synthesis Kit (Bio-Rad, 1708891) and diluted to make 10 ng/μL stock and stored at −20°C. Primers and probe sequences for droplet digital PCR (ddPCR) were as follows:

SLC43A3 (NM_014096.3) for human; Forward primer: AAG-TGATCAGCCGCTCCTTC, Reverse primer: CCAAGTAC-GGCATTCCCGAT. Universal Probe Library, Probe #9 (cat. no. 04685075001).

Western blot and immunohistochemistry analysis

Total protein lysates were extracted from tissue culture cells using Pierce IP lysis buffer (Thermo Scientific #87788) supplemented with complete mini protease inhibitor cocktail (Sigma #11836153001). The protein concentration was determined using the BCA Protein Assay Kit (Pierce). Protein (20 μg) was run on SDS-PAGE gels, transferred to PVDF membranes, and proteins were detected with rabbit polyclonal antibody for *SLC43A3* (Atlas Antibodies, HPA030551, 1:200 dilution in 5% BSA). Protein loading was determined with antibodies against beta-actin (Sigma). IHC analysis was performed on a Dako Autostainer Link 48 system. Briefly, the slides were baked for 20 minutes at 60°C, then deparaffinized and hydrated before the antigen retrieval step. Heat-induced antigen retrieval was performed at pH 6 for 20 minutes in a Dako PT Link. The tissue was incubated with a peroxidase block and then an antibody incubation (1:100 dilution, Atlas Antibodies, HPA030551) for 60 minutes. The staining was visualized using the EnVision FLEX visualization system. Pictures were taken with Hamamatsu Nanozoomer 2.0HT by using 40× objective.

γH2AX immunofluorescence staining

Tissue sections (5 μm thick) were deparaffinized and hydrated before the antigen retrieval step. Heat-induced antigen retrieval was performed at pH 6 for 20 minutes. The tissues were incubated with blocking buffer (4% BSA in 0.1% Tween-20+PBS) for 30 minutes. Sections were incubated with phospho-histone H2AX antibody (1:500, Cell Signaling Technology, cat.# 9718) in blocking buffer overnight at 4°C. Following washes with PBST, tissue sections were incubated with Alexa Flour 568–conjugated goat anti-rabbit (1:500, Invitrogen, A11011) in blocking buffer at room temperature for 1 hour. Sections were washed and mounted with Vectashield mounting medium with DAPI (Vector Laboratories), and images were taken with fluorescence microscope by using 40× objective.

Gene expression differences of 6-thio-dG–sensitive and –resistant cell lines using microarray

Gene expression differences were determined between 40 NSCLCs (the cells that had $IC_{50} \leq 1.55$ μmol/L and those cells that had $IC_{50} \geq 10$ μmol/L) by microarray analysis. Briefly, approximately 5 μg of total cellular RNA was isolated from each cell line and reverse transcribed into cDNA using standard techniques. The cDNA was indirectly labeled with a fluorescent probe using a two-step hybridization and labeling protocol where the gene chip (Illumina Human

WG-6 V3, Cat No: BD-101-0203, BD-101-0603) was hybridized to cDNA overnight, washed stringently, and then poststained with fluorescent dendrimers. After hybridization and washes, the gene chip was scanned using Illumina TotalPrep Kit (Ambion) and then arrays were scanned using Illumina Beadstation 500 BeadArray reader and data acquisitioned with Illumina BeadStudio for visualization and data mining.

Raw and processed data are available on GEO (accession GSE32036), http://www.ncbi.nlm.nih.gov/geo/query/acc.cgi?token= pfiphqkackiyubo&acc=GSE32036). Raw data were processed using default parameters of the MBCB package in R/Bioconductor. Statistically significant genes were determined using unpaired t tests with multiple testing correction via the Bonferroni method ($P < 0.01$).

Gene expression differences of 6-thio-dG–sensitive and –resistant cell lines using RNA sequencing

Two independent RNA sequencing (RNA-seq) datasets were used for analyses. For the first dataset, raw sequencing data for 42 cell lines were mapped to the human reference genome (USCS Genome hg19) using TopHat 2.0.12 (15). Gene read counts were extracted from BAM files using HT-Seq (16). Normalization and differential gene expression analyses were performed using DESeq2 (17). The second dataset is a subset of NSCLC cell lines that were in culture during experiments (H2086, H1819, H1993, H1693, H2087, and HCC4017). RNA was extracted using Qiagen's RNeasy Plus Mini Kit, and sequencing was performed by GENEWIZ on Illumina HiSeq 2500 series for cell lines used in this study. Raw data were deposited on SRA (SRP131505) and processed as outlined above. Normalized counts were used to confirm that cell lines from the second RNA-seq dataset (H2086, H1819, H1993, H1693, H2087, and HCC4017) clustered with the same cell lines in the first analysis.

no symbol or _2: dataset from first RNA-seq analysis (same cell lines, replicate). *: dataset from second independent RNA-seq analysis (replicate).

(H1993, H1993_2, H1993* / H2073, H2073_2 / H1693, H1693* / H1819, H1819* / H2086, H2086* / H2087, H2087* / HCC4017, HCC4017*).

Xenograft experiment

UT Southwestern Institutional Animal Care and Use Committee–approved animal experiments (APN 2016-101375) were conducted per institutional guidelines. Athymic NCR nu/nu female mice (~6 weeks old) were used (Charles River). Note that 3.5×10^6 H2087 sensitive and acquired resistant clones were inoculated subcutaneously into the right dorsal flanks of nude mice in 100 μL PBS. When tumors became visible (~70 mm^3), mice were divided into control and 6-thio-dG treatment groups. Animals were injected with 3 mg/kg 6-thio-dG (intraperitoneally) 5 times a week for 2 weeks in 100 μL drug solution per mouse. Tumor volumes were measured by calipers and recorded every 3 to 4 days. Tumor volumes were calculated by using the following formula: (length × width × height) × 0.5.

SLC43A3 expression and Kaplan–Meier survival curves

Clinical data for lung adenocarcinoma (LUAD) and expression data for all 33 cancer types represented in The Cancer Genome Atlas (TCGA; https://www.cancer.gov/tcga) were downloaded using the R package TCGA2STAT (18). RNASeq2 level III RSEM data were used to generate the boxplot of *SLC43A3* expression. Overall survival in patients with the highest or lowest 20% *SLC43A3* expression was evaluated by Log-rank comparison of survival

curves using Kaplan–Meier estimators computed using the R survival package (19).

Statistical analysis

Data are presented as mean values ± SD for at least 2 to 3 replicates, and significant differences between experimental conditions were determined using two-tailed unpaired t test (****, $P < 0.0001$). *In vivo* data are presented as mean values ± SEM and P value determined by two-way ANOVA. Graphs and statistical analysis used GraphPad Prism software version 7.

Results

Combining mRNA expression profiles and drug response phenotypes in NSCLC lines

We determined 6-thio-dG response phenotypes across a large panel ($n = 77$) of NSCLC lines that represent a variety of responses to clinically available drugs (Supplementary Table S1). The median IC$_{50}$ of 77 NSCLC lines was 1.55 μmol/L. Therefore, we used the median IC$_{50}$ (1.55 μmol/L) concentration to set the threshold for sensitive cell lines. A large proportion of NSCLC had IC$_{50}$ values <1.5 μmol/L (40 NSCLC lines). Only 4 of 77 NSCLC lines exhibited IC$_{50}$ values to 6-thio-dG >10 μmol/L (H1693 IC$_{50}$: 40 μmol/L, H1993 IC$_{50}$: 34 μmol/L, H2086 IC$_{50}$: 11.5 μmol/L, H1819 IC$_{50}$: 10.5 μmol/L; **Fig. 1A**) and 33 NSCLC lines fell in between these two groups. We confirmed the 6-thio-dG resistance of these 4 NSCLC
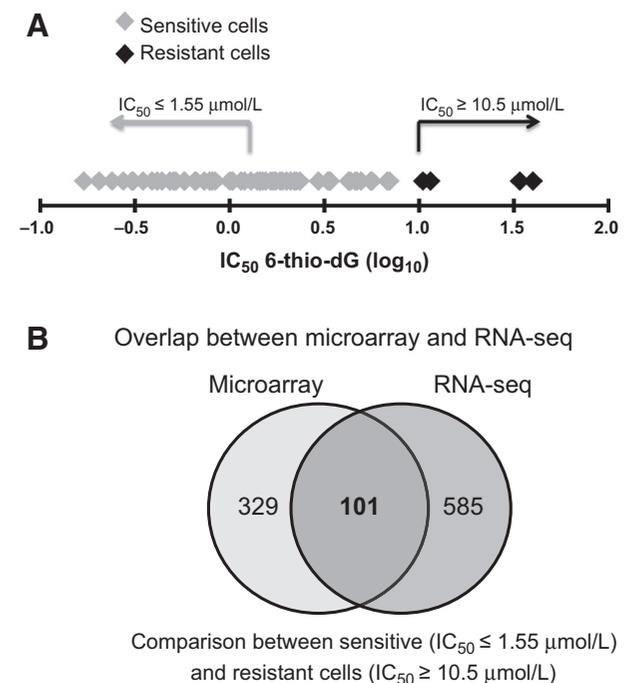

Figure 1.

A, Column scatter graph shows the IC$_{50}$ values of NSCLC cells on log$_{10}$ scale following 6-thio-dG treatment. IC$_{50}$ values of four cell lines, H1819, H2086, H1993, and H1693, were higher (IC$_{50}$ > 10 μmol/L) compared with 73 cell lines tested. Thus, only 4 of 77 NSCLC cell lines were intrinsically resistant to 6-thio-dG. For further analysis, cells IC$_{50} \leq$ 1.55 μmol/L (median) and IC$_{50}$ > 10 μmol/L selected as sensitive and resistant group, respectively. **B,** Venn diagram shows the overlap between microarray (430 genes) and RNA-seq (686) data.

Mender et al.

lines by a separate assay treating the cells with 3 μmol/L 6-thio-dG every 3 days for 1 week, and found >50% of the cells from these 4 lines survived in this treatment. We then determined genes with differential expression by stringent filtering between 6-thio-dG–sensitive and –resistant NSCLCs found in both microarray and RNA-seq analyses. Mean $\log_2$ expression of *SLC43A3* in RNA-seq data for sensitive NSCLC lines ($IC_{50} \leq 1.55$ μmol/L) was 8.603, for nonresponsive NSCLC lines ($IC_{50} \geq 10$ μmol/L) was 3.256, and for NSCLC lines that fall in between two categories is 4.574 (**Fig. 1B**; Supplementary Figs. S1 and S2).
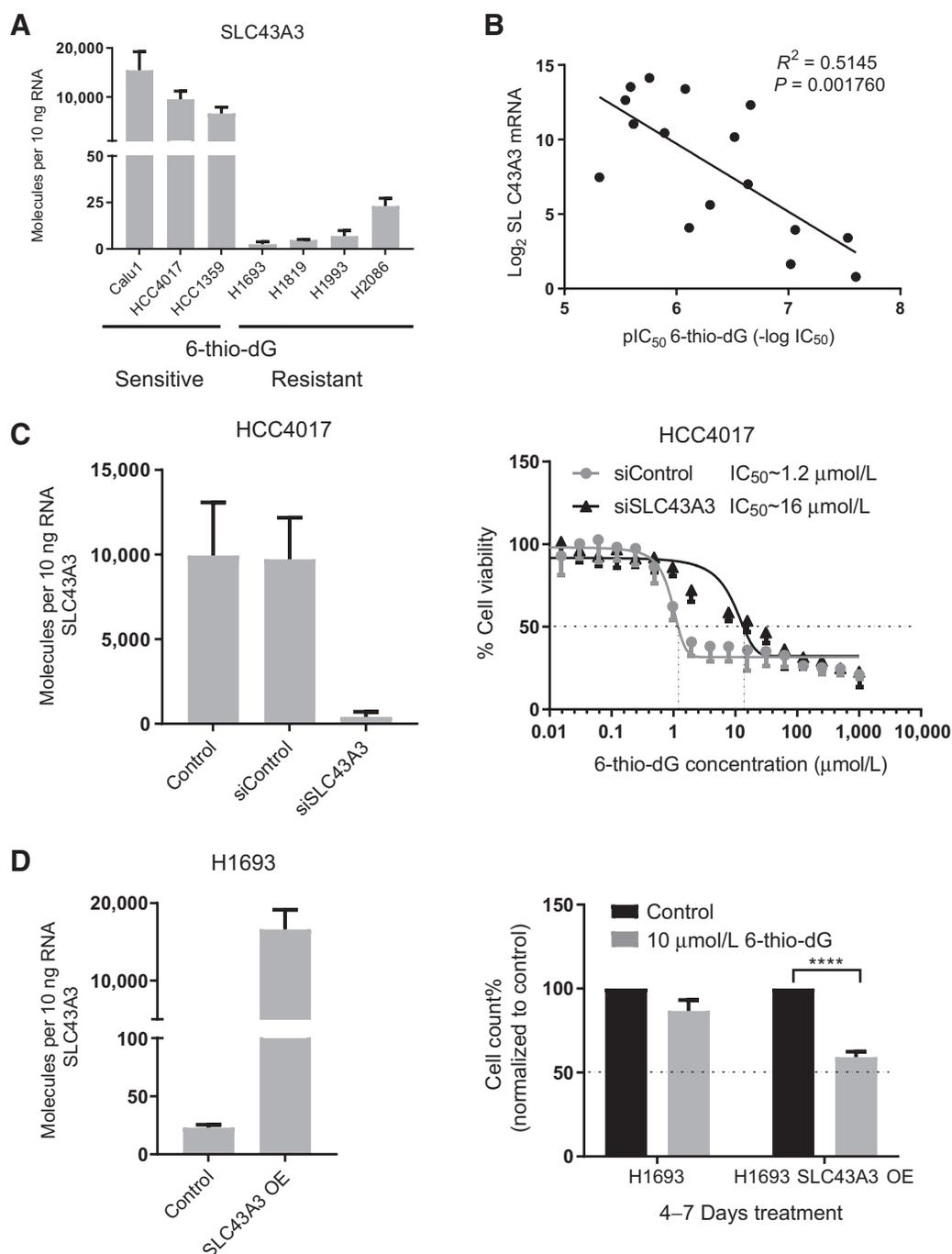

Figure 2.
A, ddPCR showing *SLC43A3* mRNA level in 6-thio-dG–sensitive and –resistant cells. **B,** Negative linear relationship between *SLC43A3* mRNA levels ($\log_2$ of molecules per 10 ng RNA) and 6-thio-dG IC_{50} values [$pIC_{50} = \log_{10}(IC_{50} \times 10^6)$] in 16 NSCLCs. **C,** Left, ddPCR showing siRNA knockdown efficiency of *SLC43A3* in HCC4017 NSCLCs. Right, knockdown of *SLC43A3* in HCC4017 shifts 6-thio-dG IC_{50} to a higher concentration. **D,** Left, ddPCR showing overexpression efficiency of *SLC43A3* in H1693 NSCLCs. Right, overexpression of *SLC43A3* in H1693 resulting in increased 6-thio-dG sensitivity following 10 μmol/L treatment.
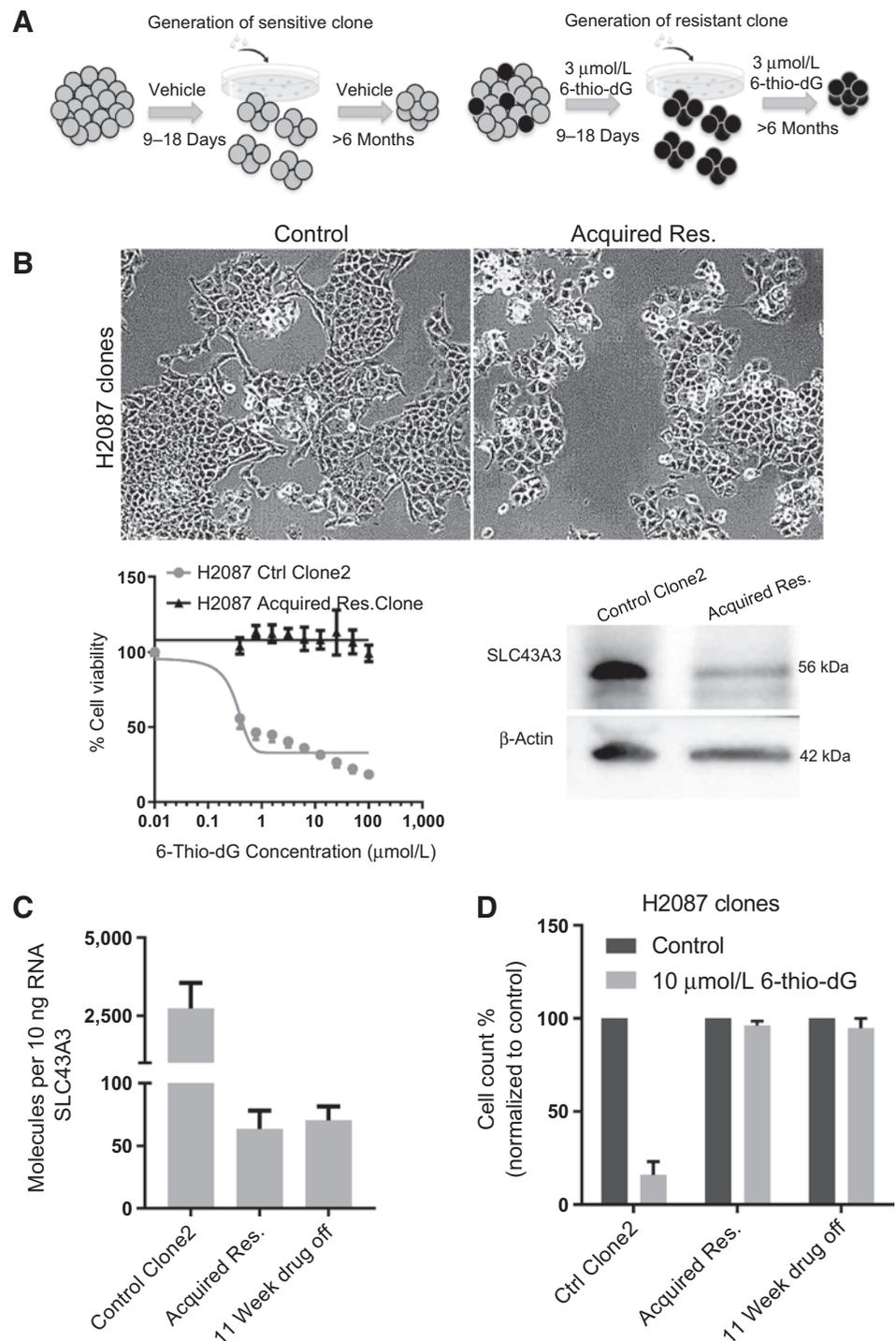
Downregulation of *SLC43A3* confers resistance to 6-thio-dG in NSCLC

Transcriptomic studies identified 101 genes that were differentially expressed between 6-thio-dG–sensitive and –resistant cell lines. We chose ten different gene candidates based on our literature search. We included *SLC29A1 (ENT1)* even though it was not present in our gene signature, because it was shown that *SLC29A1* plays a role in the transport of nucleoside analogues. However, when we knocked down *SLC29A1* in HCC4017 NSCLC, we did not observe a difference in the IC$_{50}$ of 6-thio-dG. *SLC13A3* and *SLC15A3* were other candidates of the differential expressed genes that might be involved in drug transport, but they were also eliminated as candidates. Next, we tested *SLC43A3* (solute carrier family 43 member A3) due to its function in purine transport. *SLC43A3* was significantly downregulated in 6-thio-

Figure 3.
A, Schematic figure shows the generation of sensitive and resistant clones. **B,** Brightfield image (10×) shows the morphology of sensitive and resistant clones (top plot). Left, IC$_{50}$ of H2087-sensitive and -resistant clones. Right, Western blot shows *SLC43A3* protein levels in H2087 sensitive and acquired resistant clones. β-Actin was used as a loading control. **C** and **D,** ddPCR showing *SLC43A3* gene expression level (**C**) and cell count (**D**) in H2087-sensitive, acquired resistant, and 11-week drug off clones with/without 6-thio-dG.

Mender et al.

dG–resistant NSCLC lines, which nominated it as a top candidate for conferring 6-thio-dG resistance based on differences in mRNA expression and significance between resistant and sensitive cell lines. We next validated differential *SLC43A3* mRNA levels in 6-thio-dG–sensitive

and –resistant cell lines using ddPCR. We found that although Calu1, HCC4017, and HCC1359 (sensitive cell lines) had substantially higher mRNA expression of *SLC43A3*, there was very low or no expression in H1693, H1819, H1993, and H2086 (intrinsically resistant cell

Figure 4.
A, Xenograft experiment in H2087-sensitive and acquired resistant clones (3 mg/kg 6-thio-dG, 5 times in a week for 2 weeks). **B,** *SLC43A3* mRNA level and cell viability in patient-derived cell lines. **C,** Kaplan–Meier plot of the highest and lowest 20% *SLC43A3* expression in TCGA-LUAD. **D,** Box plot of *SLC43A3* expression in the 33 cancer types in TCGA. ns, nonsignificant.

lines; **Fig. 2A**). We further investigated the relationship between *SLC43A3* mRNA expression levels and 6-thio-dG IC_{50}s of 16 NSCLC lines and found a negative correlation between the two variables (correlation coefficient, $r = -0.756$; **Fig. 2B**). We next functionally tested the role of *SLC43A3* by siRNA knockdown in 6-thio-dG–sensitive HCC4017 cells (**Fig. 2C**), that resulted in development of resistance to 6-thio-dG. In addition, overexpressing *SLC43A3* in the 6-thio-dG–resistant cell line H1693 resulted in increased 6-thio-dG cell killing (**Fig. 2D**).

To establish *in vitro* models of lung cancer acquired resistance, we treated 6-thio-dG–sensitive H2087 NSCLCs with either vehicle or 6-thio-dG (3 μmol/L) for 9 to 18 days and selected the clones that survived following vehicle or 6-thio-dG treatment. We then continued to passage the selected clones with vehicle or 6-thio-dG treatment until cells that could survive and grow in the present of 6-thio-dG (>6 months; **Fig. 3A**). We did not observe any changes in cell morphology over the course of selection, such as epithelial–mesenchymal transition (**Fig. 3B**, top plots). Cells were then characterized for their drug response. Although the H2087 original control clone was highly sensitive to 6-thio-dG treatment, 6-thio-dG did not kill the H2087 cells that were selected for growth in 6-thio-dG. We thus developed isogenic 6-thio-dG–sensitive and –resistant cell lines (**Fig. 3B**, left bottom plot). We performed Western blot (**Fig. 3B**, right bottom plot) and ddPCR (**Fig. 3C**, left plot) analyses to test *SLC43A3* protein and mRNA levels in 6-thio-dG–sensitive and acquired resistant clones and found that *SLC43A3* gene expression decreased 40-fold in the H2087 6-thio-dG–resistant compared with the sensitive clone. To determine if 6-thio-dG resistance was reversible, 6-thio-dG treatment was stopped after 6 months of treatment and cells were grown in the absence of drug for 11 weeks. After 11 weeks off 6-thio-dG, cells were still resistant and still exhibited downregulated *SLC43A3* expression level (**Fig. 3C** and **D**). Further, we compared the transcriptional profile of H2087 control and acquired resistant clones and found 154 genes that were differentially expressed by RNA-seq at $P < 0.01$ and >2 fold change. Only 5 genes (*ATP8B3, HCP5, IFITM1, SLC43A3,* and *SYT12*) came up from the overlap analysis between 154 genes and 101 differentially expressed genes, and *SLC43A3* was one of them (Supplementary Fig. S3). In addition, we performed xenograft experiments with H2087-sensitive and acquired resistant clones. We injected 3 mg/kg 6-thio-dG 5 times in a week for 2 weeks and confirmed the sensitivity and resistance to 6-thio-dG in H2087-sensitive and acquired resistant clones, respectively (**Fig. 4A**). H2087 acquired resistant and sensitive control tumors showed a correlation between IHC of *SLC43A3* and sensitivity to 6-thio-dG. Increased level of γH2AX in 6-thio-dG–treated sensitive model provided an additional evidence of mechanism-based activity (Supplementary Fig. S4A and S4B). We tested two freshly established lung tumor cell lines from patients with lung cancer (HCC4150 and HCC4087) that express high *SLC43A3* and validated *SLC43A3* mRNA levels in these two cell lines. We then determined IC_{50} of 6-thio-dG in HCC4150 (<1 μmol/L) and HCC4087 (∼1.5 μmol/L) and found both cell lines sensitive to 6-thio-dG (**Fig. 4B**). We also performed IHC in two patient-derived xenograft tumors, HCC4170 lung squamous and HCC4225 lung adenocarcinoma, which have low (expression of *SLC43A3* in RNA-seq data is 0.146) and high expression (expression of *SLC43A3* in RNA-seq data is 5.56). Our analysis showed a correlation between IHC and mRNA level of *SLC43A3* in PDX tumors (Supplementary Fig. S5). According to TCGA analyses (either with chemotherapy or without chemotherapy), low *SLC43A3* expression was associated with poor prognosis, and high *SLC43A3* expression was associated with better prognosis (**Fig. 4C**). However,

SLC43A3 is highly expressed in lung tumors compared with most other tumor types, and it may provide better therapeutic responses for patients who have high *SLC43A3* expression with progressive disease (**Fig. 4D**).

6-Thio-dG drug response of human SCLC

We determined 6-thio-dG response phenotypes across a panel of SCLCs ($n = 15$) and investigated the relationship between *SLC43A3* mRNA levels and 6-thio-dG IC_{50}s of 15 SCLC lines and found a weaker correlation between the two variables (correlation coefficient, $r = 0.0494$; Supplementary Fig. S6). In addition, we did not find many genes in SCLC RNA-seq that overlapped with NSCLC. This indicates that *SLC43A3* is more specific for NSCLC. Because the microarray and RNA-seq data were analyzed based on 6-thio-dG response profiles in NSCLC cell lines, we expected a better correlation in NSCLCs compared with SCLCs. In addition, some SCLC cells grow in suspension, some as adherent, and some as suspension+adherent in culture. Their *SLC43A3* expression profile can differ based on cell culture conditions even among SCLC cell lines.

Discussion

We used preclinical models to develop mRNA expression signatures to determine which patients with NSCLC would receive the most benefit from 6-thio-dG therapy. We reasoned that these signatures could be used as future clinical inclusion/exclusion biomarkers. Our results showed that most NSCLC cells tested were highly sensitive (≤1.55 μmol/L) to 6-thio-dG showing the broad utility of 6-thio-dG. Transcriptomic analyses of the 6-thio-dG–resistant NSCLC cell lines resulted in the reduced expression of *SLC43A3* being responsible for 6-thio-dG resistance. Human *SLC43A3* is expressed abundantly in the liver, lung, heart, and ubiquitously in the pancreas, thymus, placenta, and kidney (5, 6). However, these normal tissues are telomerase negative and thus 6-thio-dG is unlikely to adversely affect these tissues (9). Therefore, *SLC43A3* is a useful biomarker to measure patients with NSCLC in future 6-thio-dG clinical trials.

Disclosure of Potential Conflicts of Interest

Authors' Contributions

Conception and design: I. Mender, J.D. Minna, J.W. Shay
Development of methodology: I. Mender, K. Batten
Acquisition of data (provided animals, acquired and managed patients, provided facilities, etc.): I. Mender, M. Peyton, B. Gao, J.D. Minna
Analysis and interpretation of data (e.g., statistical analysis, biostatistics, computational analysis): I. Mender, K. Batten, C. Cornelius, L. Girard, J.W. Shay
Writing, review, and/or revision of the manuscript: I. Mender, K. Batten, B. Gao, J.D. Minna, J.W. Shay
Administrative, technical, or material support (i.e., reporting or organizing data, constructing databases): K. Batten, C. Cornelius, B. Gao
Study supervision: J.W. Shay
Other (analysis of data and technical support): A. Vemula
Other (grant support): J.D. Minna

Acknowledgments

Mender et al.

References

1. Burnstock G. Physiology and pathophysiology of purinergic neurotransmission. Physiol Rev 2007;87:659–797.
2. Murray AW. The biological significance of purine salvage. Annu Rev Biochem 1971;40:811–26.
3. Lane AN, Fan TW. Regulation of mammalian nucleotide metabolism and biosynthesis. Nucleic Acids Res 2015;43:2466–85.
4. Inoue K. Molecular basis of nucleobase transport systems in mammals. Biol Pharm Bull 2017;40:1130–8.
5. Bodoy S, Fotiadis D, Stoeger C, Kanai Y, Palacin M. The small SLC43 family: facilitator system l amino acid transporters and the orphan EEG1. Mol Aspects Med 2013;34:638–45.
6. Furukawa J, Inoue K, Maeda J, Yasujima T, Ohta K, Kanai Y, et al. Functional identification of SLC43A3 as an equilibrative nucleobase transporter involved in purine salvage in mammals. Sci Rep 2015;5:15057.
7. Furukawa J, Inoue K, Ohta K, Yasujima T, Mimura Y, Yuasa H. Role of equilibrative nucleobase transporter 1/SLC43A3 as a ganciclovir transporter in the induction of cytotoxic effect of ganciclovir in a suicide gene therapy with herpes simplex virus thymidine kinase. J Pharmacol Exp Ther 2017;360:59–68.
8. Seley-Radtke KL, Yates MK. The evolution of nucleoside analogue antivirals: a review for chemists and non-chemists. Part 1: early structural modifications to the nucleoside scaffold. Antiviral Res 2018;154:66–86.
9. Mender I, Gryaznov S, Dikmen ZG, Wright WE, Shay JW. Induction of telomere dysfunction mediated by the telomerase substrate precursor 6-thio-2′-deoxy-guanosine. Cancer Discov 2015;5:82–95.
10. Mender I, Gryaznov S, Shay JW. A novel telomerase substrate precursor rapidly induces telomere dysfunction in telomerase positive cancer cells but not telo-merase silent normal cells. Oncoscience 2015;2:693–5.
11. Mender I, LaRanger R, Luitel K, Peyton M, Girard L, Lai TP, et al. Telomerase-mediated strategy for overcoming non-small cell lung can-cer targeted therapy and chemotherapy resistance. Neoplasia 2018;20:826–37.
12. Sengupta S, Sobo M, Lee K, Senthil Kumar S, White AR, Mender I, et al. Induced telomere damage to treat telomerase expressing therapy-resistant pediatric brain tumors. Mol Cancer Ther 2018;17:1504–14.
13. Zhang G, Wu LW, Mender I, Barzily-Rokni M, Hammond MR, Ope O, et al. Induction of telomere dysfunction prolongs disease control of therapy-resistant melanoma. Clin Cancer Res 2018;24:4771–84.
14. Reyes-Uribe P, Adrianzen-Ruesta MP, Deng Z, Echevarria-Vargas I, Mender I, Saheb S, et al. Exploiting TERT dependency as a therapeutic strategy for NRAS-mutant melanoma. Oncogene 2018;37:4058–72.
15. Trapnell C, Williams BA, Pertea G, Mortazavi A, Kwan G, van Baren MJ, et al. Transcript assembly and quantification by RNA-Seq reveals unannotated tran-scripts and isoform switching during cell differentiation. Nat Biotechnol 2010;28:511–5.
16. Anders S, Pyl PT, Huber W. HTSeq–a Python framework to work with high-throughput sequencing data. Bioinformatics 2015;31:166–9.
17. Love MI, Huber W, Anders S. Moderated estimation of fold change and dispersion for RNA-seq data with DESeq2. Genome Biol 2014;15:550.
18. Wan YW, Allen GI, Liu Z. TCGA2STAT: simple TCGA data access for integrated statistical analysis in R. Bioinformatics 2016;32:952–4.
19. Therneau TM, Grambsch PM. Modeling survival data: extending the Cox model. New York: Springer; 2000.

Cancer Research

AAC-R American Association for Cancer Research

SLC43A3 Is a Biomarker of Sensitivity to the Telomeric DNA Damage Mediator 6-Thio-2 ′-Deoxyguanosine

Ilgen Mender, Kimberly Batten, Michael Peyton, et al.

Updated version	Access the most recent version of this article at: doi:10.1158/0008-5472.CAN-19-2257
Supplementary Material	Access the most recent supplemental material at: http://cancerres.aacrjournals.org/content/suppl/2020/01/16/0008-5472.CAN-19-2257.DC1

Cited articles	This article cites 18 articles, 4 of which you can access for free at: http://cancerres.aacrjournals.org/content/80/5/929.full#ref-list-1

E-mail alerts	Sign up to receive free email-alerts related to this article or journal.
Reprints and Subscriptions	To order reprints of this article or to subscribe to the journal, contact the AACR Publications Department at pubs@aacr.org.
Permissions	To request permission to re-use all or part of this article, use this link http://cancerres.aacrjournals.org/content/80/5/929. Click on "Request Permissions" which will take you to the Copyright Clearance Center's (CCC) Rightslink site.